Promotion of structural plasticity in area V2 of visual cortex prevents against object recognition memory deficits in aging and Alzheimer's disease rodents

Irene Navarro-Lobato[1, 2, #, †], Mariam Masmudi-Martín[1, 2, #, ‡], Manuel F. López-Aranda[1, 2, §], Juan F. López-Téllez[1, 2], Gloria Delgado[1, 2], Pablo Granados-Durán[1, 2], Celia Gaona-Romero[1, 2], Marta Carretero-Rey[1, 2], Sinforiano Posadas[1, 2], María E. Quiros-Ortega[1, 2], Zafar U. Khan[1, 2, 3, *]

https://doi.org/10.4103/1673-5374.389301

Date of submission: July 4, 2022

Date of decision: August 23, 2023

Date of acceptance: October 26, 2023

Date of web publication: November 8, 2023

From the Contents

Graphical Abstract

Increased neuronal arborization and denser spine density within visual area V2 can lead to long-lasting improvement in object recognition memory (ORM) and prevention of deficits in Alzheimer's disease (AD) mice and aging rats

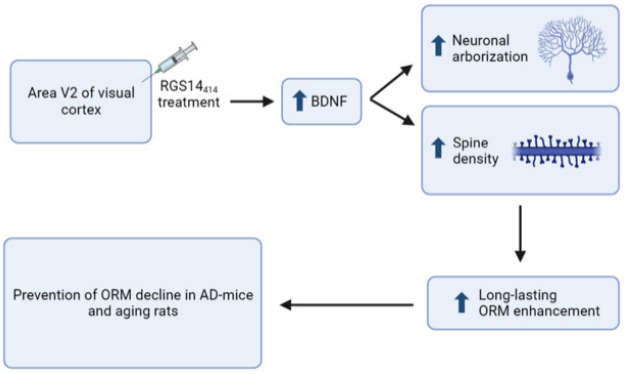

Abstract

Memory deficit, which is often associated with aging and many psychiatric, neurological, and neurodegenerative diseases, has been a challenging issue for treatment. Up till now, all potential drug candidates have failed to produce satisfactory effects. Therefore, in the search for a solution, we found that a treatment with the gene corresponding to the $RGS14_{414}$ protein in visual area V2, a brain area connected with brain circuits of the ventral stream and the medial temporal lobe, which is crucial for object recognition memory (ORM), can induce enhancement of ORM. In this study, we demonstrated that the same treatment with $RGS14_{414}$ in visual area V2, which is relatively unaffected in neurodegenerative diseases such as Alzheimer's disease, produced long-lasting enhancement of ORM in young animals and prevent ORM deficits in rodent models of aging and Alzheimer's disease. Furthermore, we found that the prevention of memory deficits was mediated through the upregulation of neuronal arborization and spine density, as well as an increase in brain-derived neurotrophic factor (BDNF). A knockdown of *BDNF* gene in $RGS14_{414}$-treated aging rats and Alzheimer's disease model mice caused complete loss in the upregulation of neuronal structural plasticity and in the prevention of ORM deficits. These findings suggest that BDNF-mediated neuronal structural plasticity in area V2 is crucial in the prevention of memory deficits in $RGS14_{414}$-treated rodent models of aging and Alzheimer's disease. Therefore, our findings of $RGS14_{414}$ gene-mediated activation of neuronal circuits in visual area V2 have therapeutic relevance in the treatment of memory deficits.

Key Words: behavioral performance; brain-derived neurotrophic factor; cognitive dysfunction; episodic memory; memory circuit activation; memory deficits; memory enhancement; object recognition memory; prevention of memory loss; regulator of G protein signaling

Introduction

Intact memory is essential for carrying out our daily life activities, such as driving in familiar environments, managing finances, remembering a grandchild's birthday, remembering to take medications, and learning to use a new computer. However, memory deficits are not only comorbid with many psychiatric, neurological, and neurodegenerative diseases but also occur in normal aging. (Bishop et al., 2010; Khan et al., 2014; Guo et al., 2019; Piolino et al., 2020). As a result, a large number of the human population is affected by this brain disease. Memory-enhancing pharmaceutical compounds are seen as a strategy for treating memory deficits or alleviating the effect of aging on memory (Bibb et al., 2010; Tampi and Jeste, 2022). However, many agents and other memory enhancers studied so far not only have failed to produce consistent and reliable effects on various types of memory but also have shown limited to no effect on memory deficits (Stern and Alberini, 2013; Dresler et al., 2019), and the search for an effective strategy is ongoing. We have previously shown that the activation of area V2 of the visual cortex by a gene corresponding to regulator of G-protein signaling 14 of 414 amino acids ($RGS14_{414}$) protein induces a long-lasting increase in object recognition memory (ORM), which is a type of episodic memory primarily affected in patients or individuals with memory deficits (López-Aranda et al., 2009; Masmudi-Martín et al., 2020, 2022). Moreover, the elimination of neurons selectively from this brain area abolishes the enhancement in ORM (López-Aranda et al., 2009). This finding further suggests that area V2 neurons play

[1]Laboratory of Neurobiology, Centro de Investigaciones Médico Sanitarias (CIMES), University of Malaga, Malaga, Spain; [2]Department of Medicine, Faculty of Medicine, University of Malaga, Malaga, Spain; [3]Centro de Investigación Biomédica en Red de Enfermedades Neurodegenerativas (CIBERNED), Institute of Health Carlos III, Madrid, Spain

†Currently at the Donders Institute for Brain Cognition and Behaviour, Radboud University, Nijmegen, The Netherlands

‡Currently at the Brain Metastasis Group, National Cancer Research Centre (CNIO), Madrid, Spain

§Currently at the Department of Neurobiology, University of California-Los Angeles, Los Angeles, CA, USA

***Correspondence to:** Zafar U. Khan, PhD, zkhan@uma.es.

https://orcid.org/0000-0003-0742-399X (Zafar U. Khan)

#These authors contributed equally to this work.

Funding: *This study was supported by grants from the Ministerio de Economía y Competitividad (BFU2013-43458-R) and Junta de Andalucía (P12-CTS-1694 and Proyexcel-00422) to ZUK.*

How to cite this article: *Navarro-Lobato I, Masmudi-Martín M, López-Aranda MF, López-Téllez JF, Delgado G, Granados-Durán P, Gaona-Romero C, Carretero-Rey M, Posadas S, Quiros-Ortega ME, Khan ZU (2024) Promotion of structural plasticity in area V2 of visual cortex prevents against object recognition memory deficits in aging and Alzheimer's disease rodents. Neural Regen Res 19(8):1835-1841.*

a crucial role in the *RGS14*$_{414}$ gene-mediated long-lasting enhancement in ORM. Previous studies have shown that neurons in the visual area V2 are interconnected with the ventral pathway, a brain circuit that originates in the visual cortex of the occipital lobe and extends to the medial temporal and frontal lobes (Khan et al., 2011; Ayzenberg and Behrmann, 2022). This ventral pathway plays a crucial role in maintaining object memory function. Therefore, the long-lasting enhancement of ORM after activation of neuronal circuits in visual area V2 by treatment with RGS14$_{414}$ may contribute to resistance to memory decline. In this study, we applied the same strategy to examine whether treatment with the *RGS14*$_{414}$ gene in visual area V2 can prevent against memory deficits in normal aging and Alzheimer's disease (AD), which are the two most extensively studied models in which memory deficits have consistently been observed (Walsh and Selkoe, 2004; Robitsek et al., 2008; Carter et al., 2020; Sasaguri et al., 2022). We further explore the underlying mechanism that drives the resistance to memory decline in these rodent models.

Methods

Animals

AD transgenic mice and rats were used in this study. The guidelines of the Institutional Animal Care and Use Committee (IACUC) of the University of Malaga were followed during the performance of all procedures. The protocols for conducting the experiments were authorized by the IACUC of University of Malaga. The approved protocols were CEUMA 32-2016-A and 7-2017-A. Animals were maintained in a temperature-regulated (20 ± 2°C) housing room under a 12-hour light/dark cycle, and drinking water and food were freely available to them. The animals were accommodated in the housing facility for at least 1 week before the commencement of the experiments, with the experiments being conducted during the light phase. All possible efforts were made to ensure the well-being and optimal health of the animals. Regular health assessments of the animals and screening for diseases and infections were conducted by departmental and veterinary staff. To minimize the pain and discomfort of animals during surgery and euthanasia, anesthesia was utilized.

Rats

In this study, we used 202 male Wistar Han rats aged 3–24 months and weighing 260 to 570 g. These rats were purchased from Charles River (Barcelona, Spain; RRID: RGD_2308816) and were housed in groups of 1 to 2 rats per cage. They were randomly assigned to three groups using the random number table method: the normal untreated group (n = 22), the vehicle group (n = 88), and the *RGS14*$_{414}$ gene group (n = 92).

Alzheimer's disease transgenic mice

In this study, we used 161 transgenic hAPPSwInd (J20) and wild-type C57BL/6J mice aged 2–10 months and weighing 18–37 g. These mice were purchased from the Jackson Laboratory (Bar Harbor, ME, USA, Stock No. 006293; RRID: MMRRC_034836-JAX) and housed 4–5 mice per cage. These mice were bred under the C57BL/6J genetic background. They were assigned to three groups using the random number table method: the normal untreated group (n = 23), the vehicle group (n = 68), and the *RGS14*$_{414}$ gene group (n = 70).

Lentivirus preparation and brain delivery

Lentivirus preparation and delivery were conducted as described previously (Masmudi-Martín et al., 2020). Briefly, the human RGS14 gene (GenBank accession number AY987041) was cloned into pLenti6/Ubc/V5-DEST Gateway vector from Thermo Fisher Scientific, Madrid, Spain (Cat# V49910), and the lentivirus containing the RGS14 gene was generated. The lentivirus containing the vehicle (control) was produced using the vector alone. For lentivirus delivery, the animals were anesthetized with sevoflurane gas (Sodispan Research SL, Madrid, Spain; 5% for anesthesia induction and 2% for anesthesia maintenance) through inhalation using a nose cone mask. Then, they were placed on a stereotaxic frame according to the coordinates provided by Paxinos and Watson (1998) and Paxinos and Franklin (2001). The coordinates for the injection in the visual area V2 of the rat brain were anterior-posterior –4.3, medial-lateral –2.1, and dorsal-ventral –1.9, and those for the mouse brain were anterior-posterior –2.3, medial-lateral –1.3, and dorsal-ventral –0.7. An aliquot of 2 µL of lentivirus from a stock titer of 2.3 × 10^7 TU/mL was injected bilaterally (1 µL in each hemisphere). The animals were left for recovery until the beginning of the experiments. In general, studies were performed 21 days after the injection. However, some behavioral studies were performed between 1–12 months after the injection. After the behavioral studies, the dissected out rat brains were processed for the evaluation of the affected surface area after the injection of lentivirus containing the RGS14$_{414}$ gene in visual area V2. Previous studies by Masmudi-Martín et al. (2020) and Navarro-Lobato et al. (2022) have revealed that RGS14$_{414}$ protein expression is restricted to visual area V2 (**Additional Figure 1**).

ORM test in rats

The ORM test was performed as previously described (López-Aranda et al., 2009; Masmudi-Martín et al., 2020; Navarro-Lobato et al., 2021). Briefly, rats were handled for 5 days, and then, they were habituated for 2 days in an open field of 100 cm × 100 cm × 50 cm dimension. In general, on the day of experiment, rats were exposed to two identical objects and after 24 hours of the object exposure, ORM status of rats were evaluated by presenting one novel object and one of the previously presented (familiar) object. However, the delay time after the object exposure was adjusted between 30 minutes and 7 days. The average total object exploration time (novel object + familiar object) during the test session of vehicle and RGS14$_{414}$ group of rats was 27.76 ± 2.93 seconds and 28.34 ± 3.17 seconds, respectively. Discrimination index (DI) was calculated by dividing the time of exploration of novel object by the total time of exploration of familiar and novel objects. The DI value equal to or less than 0.5 suggests that rats were incapable to hold information on object in memory because they explored both novel and familiar objects for equal times (novel object 50%, familiar object 50%). However, DI above to 0.66 suggests that the animals were able to successfully hold the object information in memory because they employed more than 66% of the total time in exploration of novel object and less than 34% of the time in exploration of familiar object.

ORM test in AD and wild-type mice

ORM test in AD mice was similar to as in rats except that the dimension of open field was smaller (50 cm × 35 cm × 50 cm) and the mice were exposed twice for 10 minutes during object exposure session (Masmudi-Martín et al., 2019; Navarro-Lobato et al., 2022). The object information retention test was performed 24 h after the object exposure. DI values were calculated as in rats. Average total object exploration time (novel object + familiar object) during the test session of vehicle and RGS14$_{414}$ group of AD mice was 24.71 ± 2.63 and 24.19 ± 2.28 seconds, respectively. The ORM test was performed similarly in AD mice as in rats except that the dimension of the open field was smaller (50 cm × 35 cm × 50 cm), and the mice were exposed twice for 10 minutes during the object exposure session (Masmudi-Martín et al., 2019; Navarro-Lobato et al., 2022). The object information retention test was performed 24 hours after the object exposure. The DI values were calculated as in rats. The average total object exploration time (novel object + familiar object) during the test session of vehicle and RGS14$_{414}$ group of AD mice was 24.71 ± 2.63 seconds and 24.19 ± 2.28 seconds, respectively.

Brain extraction

Prior to starting the brain extraction, animals were anesthetized through intraperitoneal injections with 75 mg/kg ketamine (as Imalgene 1000 manufactured by Merial Laboratorios and supplied by Animal Experimentation Service, Malaga, Spain) and 1 mg/kg (rats) or 0.5 mg/kg (mice) of medetomidine (as Domtor manufactured by Pfizer and supplied by Animal Experimentation Services, Malaga, Spain). After the deep sleep, the heads of those animals were separated with guillotine, and the brains were dissected out from the skull, and visual area V2 was extracted with a 4 mm punch from DH Material Médico (Barcelona, Spain, Cat# 94158BP-40F). The punches were used for quantitative reverse transcription-polymerase chain reaction (qRT-PCR) and western blot experiments.

Neuronal arborization

Neuronal arborization study was performed as previously described (Masmudi-Martín et al., 2019; Navarro-Lobato et al., 2022). Briefly, rat and mouse brains were processed for Golgi-Cox staining with a Rapid GolgiStain kit from FD Neurotechnologies (Cat# PK401; Columbia, MD, USA).180 µm thick brain sections were mounted on slide using Permount mounting medium. Neurons in the injection area (visual area V2) were examined with DM IRE2 microscope from Leica Microsystems (Barcelona, Spain) and analyzed with Leica MM AF software version 1.6.0 from Leica Microsystems. In total, 36–42 neurons from the vehicle group and 42–48 neurons from the RGS14$_{414}$ group were analyzed. Neuronal tracing, Sholl analysis for neuronal arborization, total neuronal cable length, and neuronal branching studies were done using ImageJ program (version 1.53t; National Institute of Health, Bethesda, MD, USA). Dendritic spines of pyramidal neurons were counted according to the physical appearance into the stubby, thin, and mushroom shapes (Morrison and Baxter, 2012). However, no differences were found in any of these subclasses of spine between the vehicle and RGS14$_{414}$ groups, and therefore, they were combined.

Quantitative reverse transcription-polymerase chain reaction

The quantitative reverse transcription-polymerase chain reaction (qRT-PCR) was performed as described previously (Masmudi-Martín et al., 2019; Navarro-Lobato et al., 2022). In brief, extracted rat and mouse brain punches from visual area V2 were processed for RNA extraction and cDNA synthesis from the RNA samples using the High Capacity RNA-to-cDNA kit from Applied Biosystems (Cat# 4387406). For the estimation of BDNF mRNA levels in the cDNA samples, forward (AAG CAA TAT TTC TAC GAG ACC AAG TG) and reverse (TAC GAT TGG GTA GTT CGG CAT T) primers specific to the BDNF gene were synthesized. These primers were designed to be specific to both the rat (GenBank accession number, NM_001270630.1) and mouse (GenBank accession number, NM_007540.4) BDNF genes. The qRT-PCR reaction was performed in a thermocycler 7500 Real-Time PCR System from Applied Biosystems (Fisher Scientific) and the reaction conditions were as follows: 95°C for 10 minutes for denaturation, followed by 45 cycles of 95°C for 15 seconds, and 60°C for 60 seconds. The housekeeping gene of the qRT-PCR reaction was Ribosomal protein L19 (Rpl19), and the ΔCt method was used for the determination of BDNF mRNA levels. All the values were normalized to the housekeeping gene.

Western blotting

The blots were performed as described previously (Masmudi-Martín et al., 2019; Navarro-Lobato et al., 2022). Briefly, the punches taken from the visual area V2 were homogenized in a Tris-HCl buffer containing phosphatase

and protease inhibitors (Merck Life Science, Madrid, Spain). After treating the homogenate with sodium dodecyl sulfate sample buffer, the extracted proteins in the supernatant were separated on 4–20% stain-free acrylamide gels and transferred onto polyvinylidene difluoride membranes. These membranes were then incubated at 4°C overnight with goat polyclonal anti-BDNF (pro) antibodies diluted at 1:1000. The goat anti-BDNF (pro) was obtained from Santa Cruz Biotechnology (Heidelberg, Germany, Cat# sc33904, RRID: AB_2259044). After incubation with antibodies to BDNF, the membranes were incubated with donkey anti-goat IgG-HRP at room temperature for 1 hour. Immunoreactive protein bands were developed with chemiluminescent HRP substrate (Merck, Madrid, Spain) and images of the protein bands were acquired. An analysis of protein bands was done, and the values were normalized to corresponding lane of total protein with the use of ImageLab software from BioRad (Madrid, Spain). A single immunoreactive protein band for BDNF (pro) was detected at 32 kDa (**Additional Figure 2**).

***BDNF* gene knockdown**

Adeno-associated virus (AAV) encoding small hairpin RNA (shRNA) targeting the BDNF gene in rats (GenBank accession number: NM_001270630.1) and mice (GenBank accession number: NM_007540.4) were obtained from GeneCopoeia (Heidelberg, Germany) (Cat# AA10-RSH067171-AV03-200 for rats and AA10-MSH026637-AV03-200 for mice). The control shRNA AAV particles (Cat# AC202) were also purchased from GeneCopoeia. Similar to the method described above for lentivirus preparation and brain delivery, 2 µL containing 1×10^{10} GC AAV particles of BDNF shRNA or control shRNA were injected bilaterally (1 µL in each hemisphere) into the visual area V2 of the animal brain. After 7 days of treatment with shRNA, the animals were injected with lentivirus encoding *RGS14*$_{414}$ gene. The experiments were performed 28 days after the shRNA treatment and 21 days after the RGS14$_{414}$ injection.

Statistical analysis

No statistical methods were used to predetermine sample sizes; however, our sample sizes were similar to those reported in a previous publication (Masmudi-Martín et al., 2019). The evaluators were blinded to the treatment. The GraphPad Prism 8 (GraphPad Software, San Diego, CA, USA) was used for the preparation of plots in all figures and the analysis of statistical significance.

The data in **Figures 1–5** passed the Shapiro-Wilk normality test and their *P* values ranged between 0.096 and 0.998. The Brown-Forsythe test of equality of group variances of the data showed *P* values ranging between 0.152 and 0.997. The comparison of two groups was performed with a two-tailed unpaired *t*-test, and the comparison of more than two groups with a single variable was analyzed with a one-way analysis of variance (ANOVA) followed by Tukey's *post hoc* test. However, the comparison of multiple groups with more than one variable was performed with a two-way ANOVA Sidak's *post hoc* test. The values in all the figures are represented as mean ± SEM.

Results

***RGS14*$_{414}$ gene treatment induces enhancement in object recognition memory**

RGS14$_{414}$ gene lentivirus was delivered into the visual area V2 of rat brain to induce overexpression of RGS14$_{414}$ protein. At 3 weeks after the injection, ORM test was performed to examine memory status. We found that when an object was presented for 3 minutes to untreated rats, they were able to retain the information on the object in memory after a delay period of 30 minutes and 45 minutes but not after a delay period of 24 hours (**Figure 1A**, 30 and 45 minutes *versus* 24 hours; one-way ANOVA with Tukey's *post hoc* test, $F_{(3, 44)} = 51.87$, $P < 0.0001$). However, RGS14$_{414}$-treated rats were able to retain the same object information in memory after 24 hours or even 1 week of delay period (**Figure 1A**, vehicle *versus* RGS14 at 24 hours or 1 week; two-way ANOVA with Sidak's *post hoc* test, $F_{(1, 22)} = 82.19$, $P < 0.0001$). In contrast, a treatment with saline solution, vehicle lentivirus or lentivirus of RGS12, which is another protein that belongs to the family of RGS14$_{414}$, did not produce any effect on ORM (**Additional Figure 3**), and the memory status of these animals was the same as the untreated animals (**Figure 1A**, 24 hours). Overall, our findings demonstrate that treatment with *RGS14*$_{414}$ gene significantly enhanced ORM to such an extent that it converted the short-term ORM of 45 minutes into long-term ORM, which could still be detected even after 1 week. Given the robust ORM enhancement observed after RGS14$_{414}$ treatment, we next sought to investigate how long this ORM enhancer effect persists in RGS14$_{414}$-treated rats. Animals treated with the RGS14$_{414}$ lentivirus were tested for their ORM status after 1 to 6 months of treatment. After the animals were exposed to an object, the retention of object information was evaluated in these rats after a 24-hour delay period. We observed that the RGS-mediated enhancement of ORM was similar to that in **Figure 1A** after 1 month of the treatment (**Figure 1B**, vehicle *versus* RGS14 at 1 month; two-way ANOVA with Sidak's *post hoc* test, $F_{(1, 18)} = 320.6$, $P < 0.0001$) and beyond this time frame, the memory enhancer effect was fully intact at 2 ($P < 0.0001$), 4 ($P < 0.0001$) and 6 ($P < 0.0001$) months after the *RGS14*$_{414}$ gene treatment. These results suggest that the memory enhancer effect of RGS14$_{414}$ on ORM persists for a long time.

***RGS14*$_{414}$ gene treatment prevents ORM deficits in aging rats and AD mice**

Given the long-lasting effect of *RGS14*$_{414}$ gene treatment on ORM, we next questioned whether a treatment with RGS14$_{414}$ gene in visual area V2 can in fact prevent memory deficits observed during normal aging and in Alzheimer's disease, which are the two conditions where memory deficits have invariably been observed (Walsh and Selkoe, 2004; Robitsek et al., 2008). Therefore, we used here normal aging Wistar rats and a transgenic *hAPPSwInd* mouse model of AD to determine the effect of treatment with *RGS14*$_{414}$ gene on prevention of ORM deficits. In aging rats, 6- and 12-month-old untreated rats were able to hold the object information in memory. However, a decrease in ORM was noticed in 18-month-old untreated rats, and the recognition memory capacity of these 18-month-old rats fell to a level where they failed to keep the same information in memory (**Figure 1C**, untreated 6 or 12 months *versus* untreated 18 months; one-way ANOVA with Tukey's *post hoc* test, $F_{(3, 34)} = 32.76$, $P < 0.0001$). Furthermore, RGS14414 gene treatment at 12 months of age prevented the ORM deficit seen at 18 months of age in untreated rats, and the improvement in ORM level was maintained even after reaching 24 months of age (**Figure 1C**, vehicle *versus* RGS14 at 18 and 24 months; two-way ANOVA with Sidak's *post hoc* test, $F_{(1, 20)} = 108.4$, $P < 0.0001$). Treated rats at 18 and 24 months of age with RGS14$_{414}$ performed on the ORM test in the same way as the untreated 6-month-old rats. However, in contrast to RGS14$_{414}$, the vehicle treatment had no effect at all on the ORM, and the memory levels of these rats were the same as the 18- and 24-month-old untreated aged rats.

In contrast, AD mice exhibited a significant ORM deficit at 4 months of age (**Figure 1D**, 2-month-old AD mice *versus* 4-month-old AD mice; one-way ANOVA with Tukey's *post hoc* test, $F_{(2, 30)} = 18.35$, $P < 0.0001$). Similarly to aging rats, a treatment with RGS14414 gene in visual area V2 of AD mice at 2 months of age prevented the ORM deficit seen at the age of 4 months in AD mice (**Figure 1D**, 4-month-old AD + vehicle *versus* AD + RGS14; two-way ANOVA with Sidak's *post hoc* test, $F_{(1, 21)} = 77.24$, $P < 0.0001$).

The performance level of RGS14$_{414}$-treated AD mice was the same as wild-type mice, and the ORM levels of these animals were maintained even at 10 months of age (**Figure 1D**, 10-month-old AD + vehicle *versus* AD + RGS14; two-way ANOVA with Sidak's *post hoc* test, $F_{(1, 21)} = 77.24$, $P < 0.0001$). However, treatment with vehicle had no effect on ORM, and the ORM levels of AD mice treated with vehicle were the same as untreated AD mice.

***RGS14*$_{414}$ gene treatment increases neuronal arborization**

Considering the results that RGS14$_{414}$ gene treatment not only can produce a long-lasting effect on the improvement of ORM but also can effectively prevent the occurrence of ORM deficits in both aging rats and AD mice, we speculated that the effect of RGS14$_{414}$ might be due to changes/remodeling in neuronal structures, a type of structural plasticity that has been considered to be closely related to learning and memory and synaptic plasticity (Lamprecht and LeDoux, 2004; Choi and Kaang, 2022; Goto, 2022). Therefore, aging rat brains obtained after 21 days of the RGS14$_{414}$ treatment were processed for Golgi-Cox silver staining and structural changes were analyzed. Both the pyramidal (**Figure 2A**) and nonpyramidal neurons (**Figure 2B**) of RGS14414 gene-treated rats showed robust neuronal arborization. Further, a Sholl analysis found considerably higher neuronal arbors in pyramidal (**Figure 2C**, vehicle *versus* RGS14; two-tailed unpaired *t*-test, $P < 0.0001$) as well as in nonpyramidal (**Figure 2D**, vehicle *versus* RGS14; two-tailed unpaired *t*-test, $P < 0.0001$) neurons. Accordingly, an increase in total neuronal cable length was observed in pyramidal (**Figure 2E**, vehicle *versus* RGS14; two-way ANOVA with Sidak's *post hoc* test, $F_{(1, 20)} = 64.54$, $P < 0.0001$) as well as in nonpyramidal (**Figure 2E**, vehicle *versus* RGS14; two-way ANOVA with Sidak's *post hoc* test, $F_{(1, 20)} = 64.54$, $P = 0.0039$) neurons.

Moreover, an analysis of neuronal branching in the cell bodies of non-pyramidal neurons and in the dendrites and cell bodies of pyramidal neurons showed a significant increase in pyramidal neuronal dendritic branching (**Figure 2F**, vehicle *versus* RGS14; two-way ANOVA with Sidak's *post hoc* test, $F_{(1, 30)} = 140.3$, $P < 0.0001$) and in the cell bodies of non-pyramidal neurons (**Figure 2F**, vehicle *versus* RGS14; two-way ANOVA with Sidak's *post hoc* test, $F_{(1, 30)} = 140.3$, $P < 0.0001$). However, the effect of *RGS14*$_{414}$ gene treatment was more prominent in pyramidal neurons, where an almost 2-fold increase was observed in the total neuronal cable length and the number of dendritic branching (**Figure 2E** and **F**), and the dendritic spine density was 2.2-fold higher in RGS14$_{414}$-treated rats than in rats treated with vehicle (**Figure 2G**, vehicle *versus* RGS14; two-tailed unpaired *t*-test, $P < 0.0001$).

Similar to aging rats, AD mice showed an increase in neuronal structural plasticity after treatment with *RGS14*$_{414}$ gene (**Figure 3**). We found that in both pyramidal and nonpyramidal neurons, there were considerably higher total neuronal cable length (**Figure 3A**, pyramidal neuron, vehicle *versus* RGS14; two-way ANOVA with Sidak's *post hoc* test, $F_{(1, 20)} = 91.93$, $P < 0.0001$; and Nonpyramidal neuron, vehicle *versus* RGS14; two-way ANOVA with Sidak's *post hoc* test, $F_{(1, 20)} = 91.93$, $P = 0.0009$) and neuronal branching in dendrites of pyramidal neuron (**Figure 3B**, vehicle *versus* RGS14; two-way ANOVA with Sidak's *post hoc* test, $F_{(1, 30)} = 96.10$, $P < 0.0001$) and in cell body of nonpyramidal neuron (**Figure 3B**, vehicle *versus* RGS14; two-way ANOVA with Sidak's *post hoc* test, $F_{(1, 30)} = 96.10$, $P < 0.0001$). The total number of dendritic spine density was 2-fold higher in *RGS14*$_{414}$ gene-treated AD mice (**Figure 3C**, vehicle *versus* RGS14; two-tailed unpaired *t*-test, $P < 0.0001$). Therefore, our results suggest that *RGS14*$_{414}$ gene treatment induces a robust neuronal structural plasticity and an increase in synaptic connectivity.

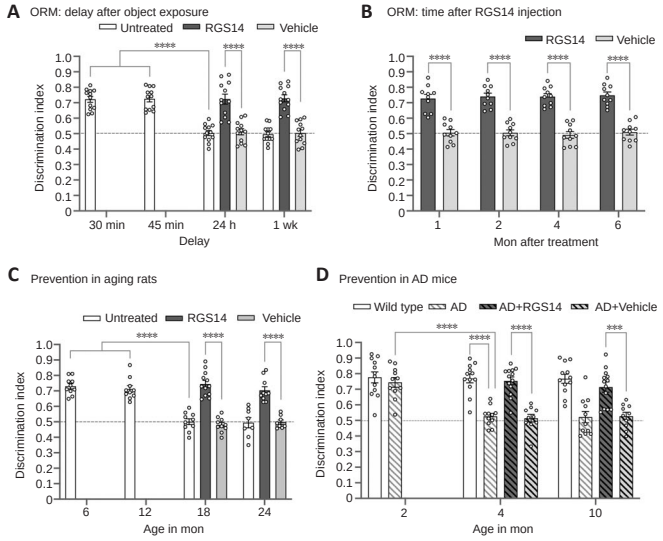

Figure 1 | ***RGS14$_{414}$* gene treatment induces ORM enhancement and prevents memory loss.**

(A) After exposure to an object, untreated 3-month-old rats were able to retain object information in memory for 30 and 45 minutes; however, they were unable to retain such information after 24 hours. *RGS14$_{414}$* gene treatment in visual area V2 of these rats induced improved ORM that was observed after 24 hours and 7 days, whereas vehicle treatment did not produce any effect. Dotted lines across panels A and B indicate the threshold at which (0.5 DI and below) the animals were unable to retain object information in memory. *n* = 12 (unfilled circles). (B) The memory-enhancing effect of *RGS14$_{414}$* gene treatment persisted for a long time in rats. *n* = 10. (C) When untreated rats aged 6 or 12 months were exposed to an object, they could retain object information in memory; however, rats aged 18 months were unable to retain this information. Injection of *RGS14$_{414}$* gene in the visual area V2 of rats aged 12 months prevented ORM loss seen at 18 months, and the memory of these RGS14$_{414}$-treated rats was maintained even after 24 months. *n* = 10–12. (D) AD mice showed substantial ORM deficits at 4 months of age compared with wild-type mice. *RGS14$_{414}$* gene injection in the visual area V2 of AD mice at 2 months of age prevented against ORM deficits observed at 4 months of age, and they showed ORM levels similar to those of wild-type mice. This level of memory was preserved at 10 months of age. *n* = 10–13. ***P < 0.001, ****P < 0.0001 (one-way analysis of variance with Tukey's *post hoc* test in A, C and D; and two-way analysis of variance with Sidak's *post hoc* test in A–D). AD: Alzheimer's disease; DI: discrimination index; ORM: object recognition memory.

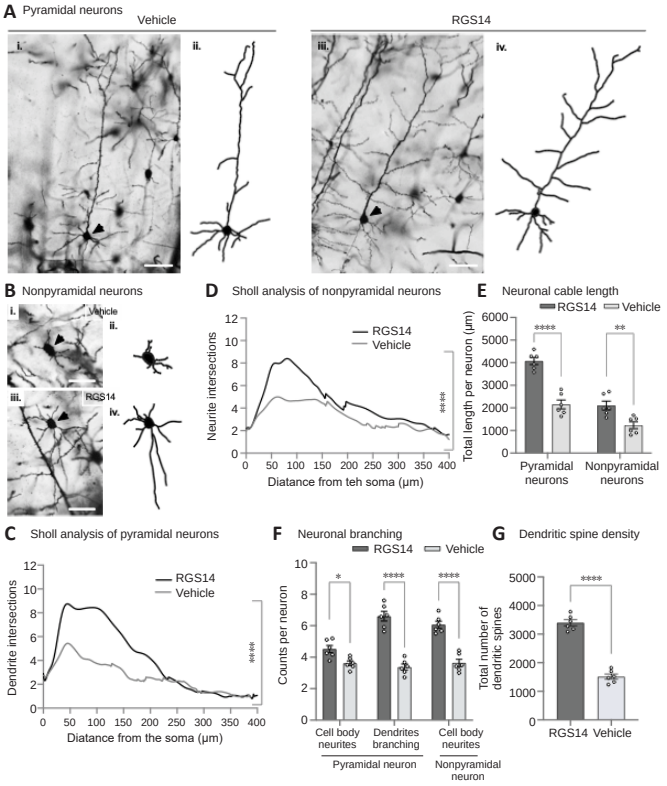

Figure 2 | ***RGS14$_{414}$* gene treatment induces neuronal arborization in aging rats.**

(A) The images of Golgi-stained pyramidal neurons from vehicle- and RGS-treated rat brain in i and iii, respectively, and in ii and iv are the respective neuronal tracings of the images in i and iii. Arrows in i and iii indicate cell body of a pyramidal neuron. Scale bars are 20 μm. (B) The images of nonpyramidal neurons in i and iii and their neuronal tracings in ii and iv. Arrows in i and iii indicate a nonpyramidal neuron. Scale bars are 10 μm. (C, D) The Sholl analysis of pyramidal and nonpyramidal neurons, respectively. Scholl analysis shows an increase in neuronal arborization in RGS14-treated rats. *n* = 6. (E) An increase in total neuronal cable length of both the pyramidal and the nonpyramidal neurons was observed in RGS14-treated rats. *n* = 6. (F) RGS14-treated animals showed an increase in the number of cell body neurites and dendritic branches in pyramidal neurons and in the cell body neurites of nonpyramidal neurons. *n* = 6. (G) Coinciding with the robust increment in dendritic branching, an upsurge in total spine number was observed in RGS-treated animals. *n* = 6. *P < 0.05, **P < 0.01, ****P < 0.0001 (two-tailed unpaired *t*-test in C, D, and G; two-way analysis of variance with Sidak's *post hoc* test in E and F).

BDNF mediates increase in the neuronal arborization and prevention in the memory deficit

Neuronal structural plasticity, which induces a long-term effect on memory, such as that in pyramidal neurons of *RGS14$_{414}$*-treated animals, has often been associated with neurotrophic factors (McAllister et al., 1999; Waterhouse and Xu, 2009; Miranda et al., 2019; Zagrebelsky et al., 2020). Therefore, we next planned to study the effect of RGS14$_{414}$ treatment on BDNF, NGF, and FGF2, which are types of neurotrophic factors related to neuronal structural plasticity and memory and are abundant in the brain.

First, the mRNA levels of these neurotrophic factors were evaluated, and then, the protein levels were determined by western blotting. The brains of aging rats and AD mice 21 days after treatment with RGS14$_{414}$ were used for the study. The qRT-PCR analysis showed an increase of 56.50 ± 4.14% in the BDNF mRNA levels in RGS-treated aging rats (**Figure 4A**, vehicle *versus* RGS14; two-way ANOVA with Sidak's *post hoc* test, $F_{(1, 20)}$ = 387.6, P < 0.0001) and 58.99 ± 4.48% in RGS-treated AD mice (**Figure 4A**, vehicle *versus* RGS14; two-way ANOVA with Sidak's *post hoc* test, $F_{(1, 20)}$ = 387.6, P < 0.0001). However, no effect on the mRNA levels of NGF and FGF2 was observed. The increase in BDNF levels observed in the qRT-PCR analysis was further confirmed by western blotting. After analyzing the optical density (OD) values of the protein bands in the western blot of **Figure 4Bii**, we found that there was an increase of 66.67 ± 3.85% in BDNF protein levels in RGS-treated aging rats (**Figure 4Bii**, vehicle *versus* RGS14; two-way ANOVA with Sidak's *post hoc* test, $F_{(1, 20)}$ = 583.9, P < 0.0001) and 65.07 ± 3.85% in RGS-treated AD mice (**Figure 4Bii**, vehicle *versus* RGS14; two-way ANOVA with Sidak's *post hoc* test, $F_{(1, 20)}$ = 583.9, P < 0.0001). This increase in BDNF in RGS-treated aging rats and AD mice indicates that RGS14$_{414}$ might mediate its effect through regulation of BDNF signaling.

The simultaneous increase in BDNF levels with the increase in neuronal arborization suggests that this protein might be involved in the neuronal structural plasticity and in the prevention of memory deficits observed in RGS-treated animals. Therefore, to evaluate the involvement of BDNF in RGS14$_{414}$-mediated prevention of memory deficits and neuronal arborization, RGS-treated aging rats and AD mice were treated with shRNA of BDNF to suppress the expression of BDNF. A treatment with BDNF shRNA reduced the BDNF expression by 70.98 ± 2.78% in aging rats (**Figure 5Ai** and **Aii**, vehicle *versus*

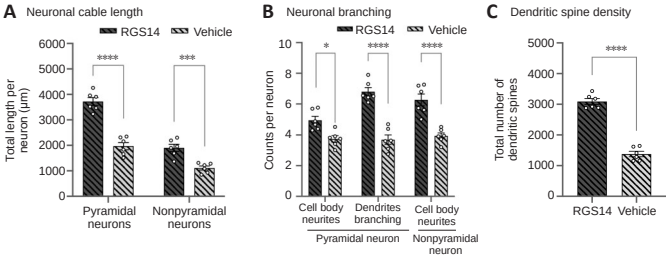

Figure 3 | ***RGS14$_{414}$* gene treatment induces neuronal arborization in AD mice.**

(A) An increase in total neuronal cable length of both the pyramidal and the nonpyramidal neurons in RGS14-treated mice. *n* = 6. (B) RGS14-treated mice showed an increase in the number of cell body neurites and dendritic branches in pyramidal neurons and of cell body neurites of nonpyramidal neurons. *n* = 6. (C) An increase in total spine number was observed in RGS-treated AD mice. *n* = 6. *P < 0.05, ***P < 0.001, ****P < 0.0001 (two-way analysis of variance with Sidak's *post hoc* test in A and B; two-tailed unpaired *t*-test in C). AD: Alzheimer's disease.

RGS14; two-way ANOVA with Sidak's *post hoc* test, $F_{(1, 20)}$ = 876.9, P < 0.0001) and by 72.41 ± 2.74% in AD mice (**Figure 5Aii**, vehicle *versus* RGS14; two-way ANOVA with Sidak's *post hoc* test, $F_{(1, 20)}$ = 876.9, P < 0.0001). Furthermore, we found that when RGS-treated aging rats and AD mice were treated with BDNF shRNA, the effect of *RGS14$_{414}$* gene treatment on the total neuronal cable length (**Figure 5B**, aging rats, RGS14 + shRNA control *versus* RGS14 + shRNA BDNF; two-way ANOVA with Tukey's *post hoc* test, $F_{(3, 40)}$ = 81.70, P < 0.0001; AD mice, RGS14 + shRNA control *versus* RGS14 + shRNA BDNF; two-way ANOVA with Tukey's *post hoc* test, $F_{(3, 40)}$ = 81.70, P < 0.0001) and dendritic branching in pyramidal neurons (**Figure 5C**, aging rats, RGS14 + shRNA control *versus* RGS14 + shRNA BDNF; two-way ANOVA with Tukey's *post hoc* test, $F_{(3, 40)}$ = 91.79, P < 0.0001 | AD mice, RGS14 + shRNA control *versus* RGS14 + shRNA BDNF; two-way ANOVA with Tukey's *post hoc* test, $F_{(3, 40)}$ = 91.79, P <

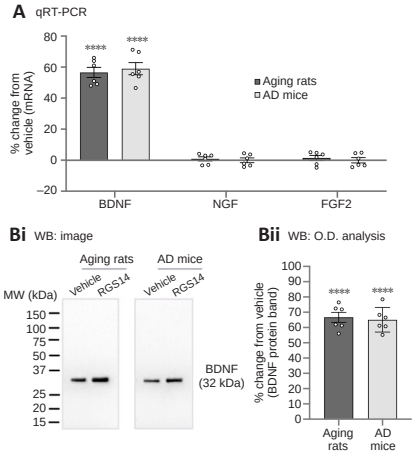

Figure 4 | ***RGS14$_{414}$* treatment causes an increase in BDNF.**
(A) qRT-PCR analysis shows that *RGS14* gene treatment increased BDNF mRNA levels but not NGF of FGF mRNA levels in both aging rats and AD mice. *n* = 6. (Bi) An example of western blots performed with brain homogenate protein from aging rats and AD mice exhibiting the expression of BDNF protein after *RGS14$_{414}$* gene treatment. (Bii) In line with the qRT-PCR results, analysis of optical density values of immunoreactive bands of BDNF protein in B.i. revealed similar level of increase in BDNF protein in RGS14-treated animals. *n* = 6 (3 experiments from each of the 2 sets of brain homogenates prepared from a pool of 4 rat brains each). ****P < 0.0001 (aging rats *versus* young rats or AD mice *versus* wild-type mice; two-way analysis of variance with Sidak's *post hoc* test; aging rats *versus* young rats). AD: Alzheimer's disease; BDNF: brain-derived neurotrophic factor; qRT-PCR: quantitative reverse transcription-polymerase chain reaction.

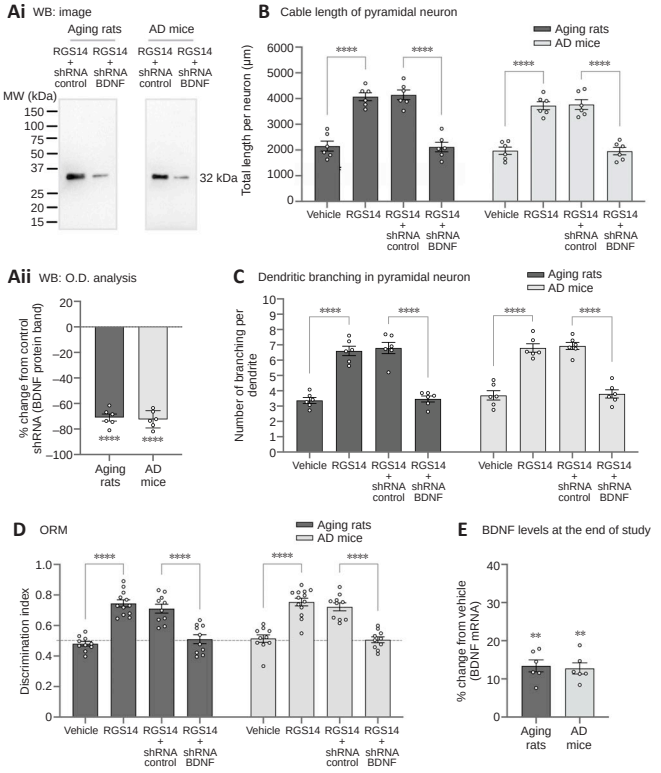

Figure 5 | **BDNF mediates the effect of RGS14$_{414}$.**
(Ai) An example of a western blot experiment using brain homogenates from animals after knocking down the BDNF gene with shRNA shows the expression of BDNF protein. (Aii) Optical density values of the immunoreactive bands of BDNF protein in A.i. showed a significant reduction in BDNF protein levels after BDNF knockdown in RGS14-treated animals. *n* = 6 (3 experiments from each of the 2 sets of brain nuclear fractions prepared from a pool of 4 rat brains each). (B, C) A knockdown of BDNF expression in both aging rats and AD mice completely abrogated the RGS14-mediated increase in total neuronal cable length (*n* = 6; B) and dendritic branching (*n* = 6; C) and (D) blocked the preventive effect of RGS14 treatment on ORM deficits (*n* = 10–13). The dotted line across the panel D indicates the threshold at which (0.5 DI and below) the animals were unable to retain object information in memory. (E) The qRT-PCR analysis results of brain tissues from aging rats and AD mice at 8 and 12 months after *RGS14$_{414}$* gene treatment, respectively. An increase in BDNF was observed even after long-term treatment; however, the level of increase was noticeably lower than the increase seen after 3 weeks of the RGS14 treatment (% change in BDNF mRNA shown in Figure 4A). *n* = 6. **P < 0.01, ****P < 0.0001 (aging rats *vs.* young rats or AD mice *vs.* wild-type mice; two-way analysis of variance with Sidak's *post hoc* test).

0.0001) completely disappeared, and these animals showed the level similar to those of control animals treated with vehicle. In addition to total neuronal length and dendritic branching, we further analyzed the effect of treatment of BDNF shRNA on the prevention of ORM deficits in RGS-treated aging rats and AD mice (**Figure 5D**). We found that when RGS-treated aging rats and AD mice were treated with BDNF shRNA, the effect of RGS14$_{414}$ on the prevention of ORM deficits was abolished (**Figure 5D**, aging rats, RGS14 + shRNA control *versus* RGS14 + shRNA BDNF; two-way ANOVA with Tukey's *post hoc* test, $F_{(3, 77)}$ = 60.80, P < 0.0001; AD mice, RGS14 + shRNA control *versus* RGS14 + shRNA BDNF; two-way ANOVA with Tukey's *post hoc* test, $F_{(3, 77)}$ = 60.80, P < 0.0001). However, in contrast to BDNF shRNA-treated animals, when RGS-treated aging rats and AD mice were treated with control shRNA, they showed no effect on the prevention of ORM deficits. A complete loss of the RGS-mediated increase in total cable length and neuronal arborization, as well as the prevention of ORM deficits after BDNF knockdown, indicates that RGS14$_{414}$ mediates its function mainly through regulation of BDNF.

At the end of the behavioral study in animals represented in **Figure 1C** and **D**, RGS14 was already administered for 12 months in aging rats and 8 months in AD mice. Therefore, we next investigated whether BDNF levels are similar in these animals compared with 3 weeks after RGS14$_{414}$ treatment shown in **Figure 4A** and **B**. We found that the BDNF levels were 13.42 ± 1.58% higher in aging rats (**Figure 5E**, vehicle *versus* RGS14; two-way ANOVA with Sidak's *post hoc* test, $F_{(1, 10)}$ = 47.46, P = 0.0016) and 12.75 ± 1.46% higher in AD mice (**Figure 5E**, vehicle *versus* RGS14; two-way ANOVA with Sidak's *post hoc* test, $F_{(1, 10)}$ = 47.46, P = 0.0011).

However, the increase in BDNF levels was noticeably lower than the increase seen after 3 weeks of the RGS14 treatment. In contrast to BDNF levels, animals at the end of study showed no difference in neuronal arborization from the animals of 3 weeks after RGS14 treatment (**Additional Figure 4**), indicating that high level of increase in BDNF is essential for neuronal arborization and low level is not.

Discussion

Our study reveals that *RGS14$_{414}$* gene treatment induced neuronal structural plasticity in both the non-pyramidal and pyramidal neurons of visual area V2, and the resistance of aging rats and AD mice to ORM deficits was associated with the induction of this area neuronal structural plasticity. Within both the inhibitory component, which is derived from non-pyramidal neurons, and the excitatory component, which is derived from pyramidal neurons, there was a similar level of structural plasticity. However, in non-pyramidal neurons, branching was predominant in cell body neurites, which are structures involved in local inhibitory circuits, while in pyramidal neurons, branching was more prevalent in dendrites, which are structures responsible for the facilitation of synaptic communication between brain areas (Spruston, 2008; Magee and Grienberger, 2020). Furthermore, a more than two-fold increase in dendritic spines is expected to induce synaptic remodeling in the interconnected networks of visual area V2. Visual area V2 is interconnected with the ventral pathway, also known as the "what" pathway, which runs from visual cortex, passes through the temporal area, perirhinal cortex, entorhinal cortex, and converges into the hippocampus; and the network this ventral pathway is dedicated to object recognition memory in the brain (Khan et al., 2011; Ayzenberg and Behrmann, 2022). Considering that the ventral pathway is involved in the processing of ORM and visual area V2 is one of the main contributors to this pathway, a modulation in the neuronal circuits of visual area V2 might have a significant impact on ORM. Memory has been shown to be critically associated with synaptic remodeling (Martin et al., 2000; Lamprecht and LeDoux, 2004; Bailey et al., 2015; Hebscher et al., 2019). Therefore, a synaptic remodeling in visual area V2 caused by the integration of newly formed spines might indeed facilitate more efficient object information processing in the ventral pathway, which can ultimately lead to superior ORM functions. It has long been thought that memory is processed through interconnected brain circuits, which are formed by the integration of various brain regions, and a slowdown in activity of these brain circuits drives to deficits in memory (Dickerson and Eichenbaum, 2010; Samson and Barnes, 2013; Guo et al., 2019; Piolino et al., 2020). Accordingly, a poor performance in memory-deficient patients has been shown to be linked to reduced activity in the neuronal networks (Daselaar et al., 2003; Dickerson and Eichenbaum, 2010). Therefore, an increased connectivity between area V2 neurons and the ventral pathway might enhance the activity of the interconnected ventral pathway network and such consistent activity within this pathway might be crucial in the resilience of RGS-treated animals against ORM deficits.

Furthermore, we observed that both the RGS14-mediated prevention of ORM deficits and the increase in neuronal arborization were dependent on BDNF signaling because a knockdown of BDNF gene abolished both effects. BDNF is essential for learning and memory and it has been shown to play a critical role in the formation of synaptic connections, neuronal branching, and structural plasticity, as well as a reduction in BDNF signaling leads to decreased dendrite growth and spine number (Waterhouse and Xu, 2009; Kowiański et al., 2018; Keifer, 2022; Navarro-Lobato et al., 2022; Wang et al., 2022). In addition, a reduced expression of the BDNF at both mRNA and protein levels has been reported in both aging and AD (Connor et al., 1997;

Michalski and Fahnestock, 2003; Qiu et al., 2020) (Numakawa and Odaka, 2022). Therefore, an upregulation in BDNF through RGS14 treatment could prevent the deterioration in BDNF signaling in both conditions. However, we observed that RGS14 caused two distinct levels of effects on BDNF increase, depending on the time frame after treatment. One was high BDNF levels (more than 65% increase), which was observed after 3 weeks of RGS14 treatment. However, the other was low BDNF levels (less than 14% increase), which was observed after several months of RGS14 treatment. Thus, it seems that our results show an active structural plasticity during the high BDNF levels stage and a lack of structural plasticity during the stage of low BDNF levels. Therefore, our results indicate that high levels of BDNF are crucial for structural plasticity. However, the lower levels of BDNF seen several months after RGS14 treatment, a period when ORM remains intact, might serve in maintaining an adequate level of BDNF signaling in aging rats and AD mice for the preservation of synaptic integrity of interconnected neuronal networks and the prevention of their deterioration. An adequate level of BDNF is necessary for the maintenance of synaptic structures and interconnected neuronal networks in the brain, and a lower level of BDNF as observed in aging and AD, could lead to the deterioration of these structures (Kowiański et al., 2018; Miranda et al., 2019; Brigadski and Leßmann, 2020). An intact synaptic structure within the neuronal networks is essential for adequate memory functions (Zagrebelsky et al., 2020; Numakawa and Odaka, 2022). On the other hand, BDNF initiates long-term potentiation (LTP), a process that has been thought to constitute cellular substrates of learning and memory, and enhances the synaptic strength in a calcium concentration-dependent manner (Kang et al., 1997; Minichiello et al., 1999; Messaoudi et al., 2002; Solinas et al., 2019; Miao et al., 2021; Miyasaka and Yamamoto, 2021). Moreover, it has been shown that BDNF-dependent increase in the number of AMPA receptors at the postsynaptic membrane promotes LTP enhancement (Derkach et al., 2007; Fortin et al., 2012; Díaz-Alonso and Nicoll, 2021; Chater and Goda, 2022; Keifer, 2022). BDNF is also essential for the sustenance of scaffolding proteins and AMPA receptor subunits at synapses during the long haul encoding of memory related information (Jourdi et al., 2003; Torquatto et al., 2019; Pereyra and Medina, 2021). Our results showed that a treatment with RGS14414 gene in visual area V2 was adequate for the prevention of ORM deficits in aging rats and AD mice, and this $RGS14_{414}$-mediated prevention was mediated through upregulation in neuronal arborization and spine density and an increase in brain-derived neurotrophic factor (BDNF).

This study has some limitations that should be considered. We have shown here that the targeting of area V2 is sufficient in the prevention of ORM deficit; however, the efficacy of such approach in other two components of episodic memory, which are spatial and temporal memories, remains to be confirmed. Additionally, BDNF-mediated neuronal proliferation seems to be essential for the prevention of ORM deficit in rodent models of aging and AD, but whether BDNF acts in conjunction with other downstream signalling molecules/pathways is unknown. Furthermore, it is essential to consider that this study has been conducted in rodent models of aging and AD, and the translational relevance of activating area V2 through a treatment with $RGS14_{414}$ gene must be proven in patients.

In summary, our study demonstrates that $RGS14_{414}$-mediated structural plasticity in visual area V2, a brain region connected to the ventral pathway, is sufficient for the prevention of recognition memory deficits in aging rats and Alzheimer's disease mice. Therefore, activation of visual area V2 neuronal circuits through treatment with $RGS14_{414}$ may have therapeutic potential in the treatment of memory deficits. Furthermore, caudal visual cortical areas in the occipital lobe are often unaffected in neurodegenerative diseases such as Alzheimer's disease, and visual area V2 may be an important brain region for memory restoration in these conditions.

Acknowledgments: *We thank Carmen Gallardo-Martínez (University of Malaga), Javier Terrón-Melguizo (University of Malaga) and Cristina Rey Blanes (University of Malaga) for technical support.*

Author contributions: *ZUK developed the overall research concept and the project. INL, MMM, MFLA, JFLT, GD, PGD, and ZUK designed the experiments. MMM, INL, MFLA, JFLT, GD, PGD, and CGR performed the experiments. MCR, SP, and MEQO assisted with the experiments. MMM, INL, MFLA, and ZUK wrote the manuscript. All authors approved the final version of the manuscript.*

Conflicts of interest: *The authors declare no competing interests.*

Data availability statement: *All data relevant to the study are included in the article or uploaded as Additional files.*

Additional files:

Additional Figure 1: *$RGS14_{414}$ protein expression was confined to the area V2 of the visual cortex.*

Additional Figure 2: *Antibodies to brain-derived neurotrophic factor (BDNF) used to detect a single-band of the expected size in Western blots of normal rat brains.*

Additional Figure 3: *Treatment of the perirhinal cortex with vehicle, saline or RGS12 caused no effect on object recognition memory.*

Additional Figure 4: *Neuronal total cable length was unchanged after 21 days of RGS14414 treatment.*

References

Ayzenberg V, Behrmann M (2022) Does the brain's ventral visual pathway compute object shape. Trends Cogn Sci 26:1119-1132.

Bailey CH, Kandel ER, Harris KM (2015) Structural components of synaptic plasticity and memory consolidation. Cold Spring Harb Perspect Biol 7:a021758.

Bibb JA, Mayford MR, Tsien JZ, Alberini CM (2010) Cognition enhancement strategies. J Neurosci 30:14987-14992.

Bishop NA, Lu T, Yankner BA (2010) Neural mechanisms of ageing and cognitive decline. Nature 464:529–535.

Brigadski T, Leßmann V (2020) The physiology of regulated BDNF release. Cell Tissue Res 382:15-45.

Carter CS, Richardson A, Huffman DM, Austad S (2020) Bring Back the Rat. J Gerontol A Biol Sci Med Sci 75:405-415.

Chater TE, Goda Y (2022) The shaping of AMPA receptor surface distribution by neuronal activity. Front Synaptic Neurosci 14:833782.

Choi DI, Kaang BK (2022) Interrogating structural plasticity among synaptic engrams. Curr Opin Neurobiol 75:102552.

Connor B, Young D, Yan Q, Faull RL, Synek B, Dragunow M (1997) Brain-derived neurotrophic factor is reduced in Alzheimer's disease. Brain Res Mol Brain Res 49:71-81.

Daselaar SM, Veltman DJ, Rombouts SA, Raaijmakers JG, Jonker C (2003) Deep processing activates the medial temporal lobe in young but not in old adults. Neurobiol Aging 24:1005-1011.

Derkach VA, Oh MC, Guire ES, Soderling TR (2007) Regulatory mechanisms of AMPA receptors in synaptic plasticity. Nat Rev Neurosci 8:101-113.

Díaz-Alonso J, Nicoll RA (2021) AMPA receptor trafficking and LTP: Carboxy-termini, amino-termini and TARPs. Neuropharmacology 197:108710.

Dickerson BC, Eichenbaum H (2010) The episodic memory system: neurocircuitry and disorders. Neuropsychopharmacology 35:86-104.

Dresler M, Sandberg A, Bublitz C, Ohla K, Trenado C, Mroczko-Wąsowicz A, Kühn S, Repantis D (2019) Hacking the brain: dimensions of cognitive enhancement. ACS Chem Neurosci 10:1137-1148.

Fortin DA, Srivastava T, Dwarakanath D, Pierre P, Nygaard S, Derkach VA, Soderling TR (2012) Brain-derived neurotrophic factor activation of CaM-kinase kinase via transient receptor potential canonical channels induces the translation and synaptic incorporation of GluA1-containing calcium-permeable AMPA receptors. J Neurosci 32:8127-8137.

Goto A (2022) Synaptic plasticity during systems memory consolidation. Neurosci Res 183:1-6.

Guo JY, Ragland JD, Carter CS (2019) Memory and cognition in schizophrenia. Mol Psychiatry 24:633-642.

Hebscher M, Wing E, Ryan J, Gilboa A (2019) Rapid cortical plasticity supports long-term memory formation. Trends Cogn Sci 23:989-1002.

Jourdi H, Iwakura Y, Narisawa-Saito M, Ibaraki K, Xiong H, Watanabe M, Hayashi Y, Takei N, Nawa H (2003) Brain-derived neurotrophic factor signal enhances and maintains the expression of AMPA receptor-associated PDZ proteins in developing cortical neurons. Dev Biol 263:216-230.

Kang H, Welcher AA, Shelton D, Schuman EM (1997) Neurotrophins and time: different roles for TrkB signaling in hippocampal long-term potentiation. Neuron 19:653-664.

Keifer J (2022) Regulation of AMPAR trafficking in synaptic plasticity by BDNF and the impact of neurodegenerative disease. J Neurosci Res 100:979-991.

Khan ZU, Martín-Montañez E, Baxter MG (2011) Visual perception and memory systems: from cortex to medial temporal lobe. Cell Mol Life Sci 68:1737-1754.

Khan ZU, Martín-Montañez E, Navarro-Lobato I, Muly EC (2014) Memory deficits in aging and neurological diseases. Prog Mol Biol Transl Sci 122:1-29.

Kowiański P, Lietzau G, Czuba E, Waśkow M, Steliga A, Moryś J (2018) BDNF: a key factor with multipotent impact on brain signaling and synaptic plasticity. Cell Mol Neurobiol 38:579-593.

Lamprecht R, LeDoux J (2004) Structural plasticity and memory. Nat Rev Neurosci 5:45-54.

López-Aranda MF, López-Téllez JF, Navarro-Lobato I, Masmudi-Martín M, Gutiérrez A, Khan ZU (2009) Role of layer 6 of V2 visual cortex in object-recognition memory. Science 325:87-89.

Magee JC, Grienberger C (2020) Synaptic plasticity forms and functions. Annu Rev Neurosci 43:95-117.

Martin SJ, Grimwood PD, Morris RG (2000) Synaptic plasticity and memory: an evaluation of the hypothesis. Annu Rev Neurosci 23:649-711.

Masmudi-Martín M, Navarro-Lobato I, Khan ZU (2022) Implication of 14-3-3ζ-BDNF pathway in long-lasting memory enhancement and the rescue from memory deficits. Neural Regen Res 17:2685-2686.

Masmudi-Martín M, Navarro-Lobato I, López-Aranda MF, Browning PGF, Simón AM, López-Téllez JF, Jiménez-Recuerda I, Martín-Montañez E, Pérez-Mediavilla A, Frechilla D, Baxter MG, Khan ZU (2020) Reversal of object recognition memory deficit in perirhinal cortex-lesioned rats and primates and in rodent models of aging and Alzheimer's diseases. Neuroscience 448:287-298.

Masmudi-Martín M, Navarro-Lobato I, López-Aranda MF, Delgado G, Martín-Montañez E, Quiros-Ortega ME, Carretero-Rey M, Narváez L, Garcia-Garrido MF, Posadas S, López-Téllez JF, Blanco E, Jiménez-Recuerda I, Granados-Durán P, Paez-Rueda J, López JC, Khan ZU (2019) RGS14414 treatment induces memory enhancement and rescues episodic memory deficits. FASEB J 33:11804-11820.

McAllister AK, Katz LC, Lo DC (1999) Neurotrophins and synaptic plasticity. Annu Rev Neurosci 22:295-318.

Messaoudi E, Ying S-W, Kanhema T, Croll SD, Bramham CR (2002) Brain-derived neurotrophic factor triggers transcription-dependent, late phase long-term potentiationin vivo. J Neurosci 22:7453-7461.

Miao HH, Miao Z, Pan JG, Li XH, Zhuo M (2021) Brain-derived neurotrophic factor produced long-term synaptic enhancement in the anterior cingulate cortex of adult mice. Mol Brain 14:140.

Michalski B, Fahnestock M (2003) Pro-brain-derived neurotrophic factor is decreased in parietal cortex in Alzheimer's disease. Brain Res Mol Brain Res 111:148-154.

Minichiello L, Korte M, Wolfer D, Kühn R, Unsicker K, Cestari V, Rossi-Arnaud C, Lipp HP, Bonhoeffer T, Klein R (1999) Essential role for TrkB receptors in hippocampus-mediated learning. Neuron 24:401-414.

Miranda M, Morici JF, Zanoni MB, Bekinschtein P (2019) Brain-derived neurotrophic factor: a key molecule for memory in the healthy and the pathological brain. Front Cell Neurosci 13:363.

Miyasaka Y, Yamamoto N (2021) Neuronal activity patterns regulate brain-derived neurotrophic factor expression in cortical cells via neuronal circuits. Front Neurosci 15:699583.

Morrison JH, Baxter MG (2012) The ageing cortical synapse: hallmarks and implications for cognitive decline. Nat Rev Neurosci 13:240-250.

Navarro-Lobato I, Masmudi-Martín M, Quiros-Ortega ME, Gaona-Romero C, Carretero-Rey M, Rey Blanes C, Khan ZU (2021) 14-3-3ζ is crucial for the conversion of labile short-term object recognition memory into stable long-term memory. J Neurosci Res 99:2305-2317.

Navarro-Lobato I, Masmudi-Martín M, López-Aranda MF, Quiros-Ortega ME, Carretero-Rey M, Garcia-Garrido MF, Gallardo-Martínez C, Martín-Montañez E, Gaona-Romero C, Delgado G, Torres-Garcia L, Terrón-Melguizo J, Posadas S, Muñoz LR, Rios CV, Zoidakis J, Vlahou A, López JC, Khan ZU (2022) RGS14414-mediated activation of the 14-3-3ζ in rodent perirhinal cortex induces dendritic arborization, an increase in spine number, long-lasting memory enhancement, and the prevention of memory deficits. Cereb Cortex 32:1894-1910.

Numakawa T, Odaka H (2022) The role of neurotrophin signaling in age-related cognitive decline and cognitive diseases. Int J Mol Sci 23:7726.

Paxinos G, Watson C (1998) The rat brain in stereotaxic coordinates, 4th ed. New York: Academic Press.

Paxinos G, Franklin KBJ (2001) The mouse brain in stereotaxic coordinates. San Diego (CA): Academic Press.

Pereyra M, Medina JH (2021) AMPA receptors: a key piece in the puzzle of memory retrieval. Front Hum Neurosci 15:729051.

Piolino P, Bulteau C, Jambaqué I (2020) Memory dysfunctions. Handb Clin Neurol 174:93–110.

Qiu LL, Pan W, Luo D, Zhang GF, Zhou ZQ, Sun XY, Yang JJ, Ji MH (2020) Dysregulation of BDNF/TrkB signaling mediated by NMDAR/Ca2+/calpain might contribute to postoperative cognitive dysfunction in aging mice. J Neuroinflammation 17:23.

Robitsek RJ, Fortin NJ, Koh MT, Gallagher M, Eichenbaum H (2008) Cognitive aging: a common decline of episodic recollection and spatial memory in rats. J Neurosci 28:8945-8954.

Samson RD, Barnes CA (2013) Impact of aging brain circuits on cognition. Eur J Neurosci 37:1903-1915.

Sasaguri H, Hashimoto S, Watamura N, Sato K, Takamura R, Nagata K, Tsubuki S, Ohshima T, Yoshiki A, Sato K, Kumita W, Sasaki E, Kitazume S, Nilsson P, Winblad B, Saito T, Iwata N, Saido TC (2022) Recent advances in the modeling of Alzheimer's disease. Front Neurosci 16:807473.

Solinas SMG, Edelmann E, Leßmann V, Migliore M (2019) A kinetic model for brain-derived neurotrophic factor mediated spike timing-dependent LTP. PLoS Comput Biol 15:e1006975.

Spruston N (2008) Pyramidal neurons: dendritic structure and synaptic integration. Nat Rev Neurosci 9:206-221.

Stern SA, Alberini CM (2013) Mechanisms of memory enhancement. Wiley Interdiscip Rev Syst Biol Med 5:37-53.

Tampi RR, Jeste DV (2022) Dementia is more than memory loss: neuropsychiatric symptoms of dementia and their nonpharmacological and pharmacological management. Am J Psychiatry 179:528-543.

Torquatto KI, Menegolla AP, Popik B, Casagrande MA, de Oliveira Alvares L (2019) Role of calcium-permeable AMPA receptors in memory consolidation, retrieval and updating. Neuropharmacology 144:312-318.

Walsh DM, Selkoe DJ (2004) Deciphering the molecular basis of memory failure in Alzheimer's disease. Neuron 44:181-193.

Wang CS, Kavalali ET, Monteggia LM (2022) BDNF signaling in context: From synaptic regulation to psychiatric disorders. Cell 185:62-76.

Waterhouse EG, Xu B (2009) New insights into the role of brain-derived neurotrophic factor in synaptic plasticity. Mol Cell Neurosci 42:81-89.

Zagrebelsky M, Tacke C, Korte M (2020) BDNF signaling during the lifetime of dendritic spines. Cell Tissue Res 382:185-199.

C-Editor: Zhao M; S-Editor: Li CH; L-Editor: Song LP; T-Editor: Jia Y